JOURNAL OF THE KOREAN ASTRONOMICAL SOCIETY
39: 95 ~ 105, 2006

COSMIC RAY ACCELERATION AT BLAST WAVES FROM TYPE Ia SUPERNOVAE

HYESUNG KANG
Department of Earth Sciences, Pusan National University, Pusan 609 -735, Korea
E-mail: hskang@pusan.ac.kr
(Received November 10, 2006; Accepted December 6, 2006)

ABSTRACT

We have calculated the cosmic ray (CR) acceleration at young remnants from Type Ia supernovae expanding into a uniform interstellar medium (ISM). Adopting quasi-parallel magnetic fields, gasdynamic equations and the diffusion convection equation for the particle distribution function are solved in a comoving spherical grid which expands with the shock. Bohm-type diffusion due to self-excited Alfvén waves, drift and dissipation of these waves in the precursor and thermal leakage injection were included. With magnetic fields amplified by the CR streaming instability, the particle energy can reach up to $10^{16}Z$ eV at young supernova remnants (SNRs) of several thousand years old. The fraction of the explosion energy transferred to the CR component asymptotes to 40-50 % by that time. For a typical SNR in a warm ISM, the accelerated CR energy spectrum should exhibit a concave curvature with the power-law slope flattening from 2 to 1.6 at $E \gtrsim 0.1$ TeV.

Key words : cosmic ray acceleration – supernova remnants – hydrodynamics – methods:numerical

I. INTRODUCTION

Diffusive shock acceleration (DSA) is widely accepted as the primary mechanism through which cosmic rays are generated in a wide range of astrophysical shocks (Drury, 1983; Malkov & Drury 2001 and references therein; Kang & Jones 2002; Kang 2003). It is well known that the CR energy density is comparable to the gas thermal energy density in the ISM and plays important dynamical roles in the evolution of our Galaxy. Most of galactic cosmic rays, at least up to 10^{14} eV of the proton energy, are believed to be accelerated by SNRs within our Galaxy via Fermi first order process (Blanford & Ostriker 1978; Lagage & Cesarsky 1983; Blandford & Eichler 1987; Drury *et al.* 2001).

Time-dependent, kinetic simulations of the CR acceleration at SNRs have shown that up to 50 % of explosion energy can be converted to CRs, when a fraction $10^{-4} - 10^{-3}$ of incoming thermal particles are injected into the CR population at the subshock (*e.g.*, Berezhko, Ksenofontov, & Yelshin 1995; Berezhko, & Völk 1997; Völk & Berezhko 2005; Kang & Jones 2006). This should be enough to replenish the galactic CRs escaping from our Galaxy with $L_{CR} \sim 10^{41}$erg s^{-1}. X-ray observations of young SNRs such as SN1006 and Cas A indicate the presence of TeV electrons emitting nonthermal synchrotron emission immediately inside the outer SNR shock (Koyama *et al.* 1995; Bamba *et al.* 2003). They provide clear evidences for the efficient acceleration of the CR electrons at SNR shocks. Also recent HESS observation of SNR RXJ1713.7-3946 indicates possible detections of π^0 decay γ rays from the hadronic CRs accelerated by the SNR shock (Aharonian *et al.* 2004; Berezhko & Völk 2006).

In the kinetic equation approach to numerical study of CR acceleration at shocks, the diffusion-convection equation for the particle momentum distribution, $f(p)$, is solved along with suitably modified gasdynamic equations (*e.g.*, Kang & Jones 1991). Accurate solutions to the CR diffusion-convection equation require a computational grid spacing significantly smaller than the particle diffusion length, $\Delta x \ll x_d(p) = \kappa(p)/u_s$, where $\kappa(p)$ is diffusion coefficient and u_s is the shock speed. In a realistic diffusion transport model, the diffusion coefficient has a steep momentum dependence, $\kappa(p) \propto p^s$, with $s \sim 1 - 2$. So a wide range of length scales is required to be resolved in order to follow the CR acceleration from the injection energy (typically $p_{\rm inj}/m_{\rm p}c \sim 10^{-2}$) to highly relativistic energy ($p/m_{\rm p}c \gg 1$). This constitutes an extremely challenging numerical task, requiring rather extensive computational resources.

To overcome this numerical problem, Berezhko and collaborators (*e.g.*, Berezhko *et al.* 1995) introduced a "change of variables technique" in which the radial coordinate is normalized by the diffusion length, $x_d(p)$, at each particle momentum for the upstream region. This allowed them to solve the coupled system of gasdynamic equations and the CR transport equation with $\kappa(p) \propto p$. Their scheme was designed for simulations of supernova remnants, which were represented by piston-driven spherical shocks in one-dimensional (1D) spherical geometry.

On the other hand, Kang and collaborators have taken an alternative approach that is based on a more conventional Eulerian formalism. Adaptive Mesh Refinement (AMR) technique and subgrid shock tracking technique were combined to build CRASH (Cosmic-

Ray Amr SHock) code in 1D plane-parallel geometry (Kang *et al.* 2001) and in 1D spherical symmetric geometry (Kang & Jones 2006). In order to implement the shock tracking and AMR techniques effectively in a spherical geometry, we solve the fluid and diffusion-convection equations in a frame comoving with the outer spherical shock. Adopting a comoving frame turns out to be a great numerical success, since we can achieve numerical convergence at a grid resolution much coarser than that required in an Eulerian grid. In the comoving grid, the shock remains at the same location, so the compression rate is applied consistently to the CR distribution at the subshock, resulting in much more accurate and efficient low energy CR acceleration.

In the present paper, we apply the spherical CRASH code for the CR acceleration at remnant shocks from Type Ia SNe expanding into a uniform interstellar medium, assuming a quasi-parallel field geometry. Details of the numerical method are described in §II. The simulation results are presented and discussed in §III, followed by a summary in §IV.

II. NUMERICAL METHOD

(a) BASIC EQUATION

Here we consider the CR acceleration at a quasi-parallel shock where the magnetic field lines are parallel to the shock normal. So we solve the standard gasdynamic equations with CR pressure terms added in the Eulerian formulation for one dimensional spherical symmetric geometry.

$$\frac{\partial \rho}{\partial t} + \frac{\partial}{\partial r}(\rho u) = -\frac{2}{r}\rho u, \tag{1}$$

$$\frac{\partial (\rho u)}{\partial t} + \frac{\partial}{\partial r}(\rho u^2 + P_g + P_c) = -\frac{2}{r}\rho u^2, \tag{2}$$

$$\frac{\partial (\rho e_g)}{\partial t} + \frac{\partial}{\partial r}(\rho e_g u + P_g u) = -u\frac{\partial P_c}{\partial r} - \frac{2}{r}(\rho e_g u + P_g u), \tag{3}$$

$$\frac{\partial S}{\partial t} + \frac{\partial}{\partial r}(Su) = -\frac{2}{r}Su + \frac{(\gamma_g - 1)}{\rho^{\gamma_g - 1}}\left[W(r,t) - L(r,t)\right], \tag{4}$$

where P_g and P_c are the gas and the CR pressure, respectively, $e_g = P_g/[\rho(\gamma_g - 1)] + u^2/2$ is the total energy of the gas per unit mass. The evolution of a modified entropy, $S = P_g/\rho^{\gamma_g - 1}$, is followed everywhere except across the subshock, since for strongly shocked flows numerical errors in computing the gas pressure from the total energy can lead to spurious entropy generation with standard methods, especially in the shock precursor (Kang, Jones, & Gieseler 2002). Total energy conservation is applied only across the subshock. The remaining variables, except for L and W, have standard meanings. The injection energy loss term, $L(r,t)$, accounts for the energy carried by the suprathermal particles injected into the CR component at the subshock. Gas heating due to Alfvén wave dissipation in the upstream region is represented by the term

$$W(r,t) = -v_A\frac{\partial P_c}{\partial r}, \tag{5}$$

where $v_A = B/\sqrt{4\pi\rho}$ is the Alfvén speed. This term derives from a simple model in which Alfvén waves are amplified by streaming CRs and dissipated locally as heat in the precursor region (*e.g.,* Jones 1993).

The CR population is evolved by solving the diffusion-convection equation,

$$\frac{\partial g}{\partial t} + (u + u_w)\frac{\partial g}{\partial r} = \frac{1}{3r^2}\frac{\partial}{\partial r}\left[r^2(u + u_w)\right]\left(\frac{\partial g}{\partial y} - 4g\right) + \frac{1}{r^2}\frac{\partial}{\partial r}\left[r^2\kappa(r,y)\frac{\partial g}{\partial r}\right], \tag{6}$$

where $g = p^4 f$, with $f(p,r,t)$ the pitch angle averaged CR distribution, and $y = \ln(p)$, while $\kappa(r,y)$ is the diffusion coefficient parallel to the field lines (Skilling 1975). For simplicity we express the particle momentum, p in units $m_p c$ hereafter and consider only the proton CR component. The wave speed is set to be $u_w = v_A$ in the upstream region, while we use $u_w = 0$ in the downstream region. This term reflects the fact that the scattering by Alfvén waves tends to isotropize the CR distribution in the wave frame rather than the gas frame.

(b) Spherical CRASH code

Details of the CRASH code in 1D spherical symmetric geometry can be found in Kang & Jones (2006), so we briefly describe the basic features here. We solve the equations (1)-(6) in a comoving frame that expands with the instantaneous shock speed, since a spherical shock can be made to be stationary by adopting comoving variables which factor out a uniform expansion or contraction. Because the shock is at rest and tracked accurately as a true discontinuity, we can refine the region around the gas subshock at an arbitrarily fine level. The AMR technique allows us to "zoom in" inside the precursor structure with a hierarchy of small, refined grid levels applied around the shock. The result is an enormous savings in both computational time and data storage over what would be required to solve the problem using more traditional methods on a single fine grid.

(c) The Thermal Leakage Injection Model

The injection rate with which suprathermal particles are injected into CRs at the subshock depends in general upon the shock Mach number, field obliquity angle, and strength of Alfvén turbulence responsible for scattering. The CRASH codes treat this process naturally and self-consistently via "thermal leakage" through

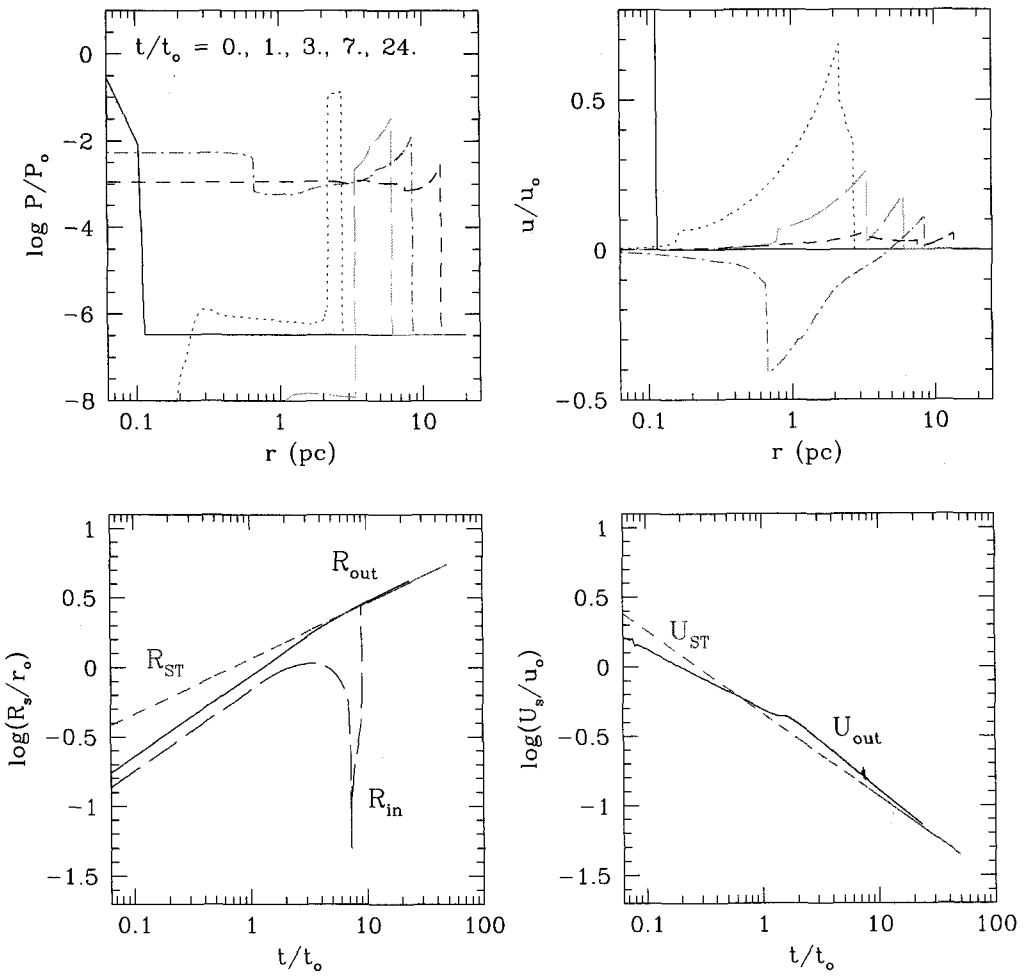

Fig. 1.— Top two panels show the evolution of a typical SNR in a gasdynamic simulation. Bottom two panels show the positions of the outer forward shock ($R_{\rm out}$) and inner reverse shock ($R_{\rm in}$) and the speed of the outer shock ($U_{\rm out}$) as a function of time. The Sedov Taylor similarity solutions for the outer shock, $R_{\rm ST}$ and $U_{\rm ST}$ are also shown for comparison.

lowest momentum bins. The thermal leakage injection model emulates the process by which suprathermal particles well into the tail of the postshock Maxwellian distribution leak upstream across a quasi-parallel shock (Malkov & Völk 1998; Malkov & Drury 2001). This filtering process is implemented numerically by adopting a "transparency function", $\tau_{\rm esc}(\epsilon_B, v)$, that expresses the probability of supra-thermal particles at a given velocity, v, leaking upstream through the postshock MHD waves (Kang *et al.* 2002). One free parameter controls this function; namely, $\epsilon_B = B_0/B_\perp$, which is the inverse ratio of the amplitude of the postshock MHD wave turbulence $B_\perp$ to the general magnetic field aligned with the shock normal, B_0 (Malkov & Völk 1998). Plasma hybrid simulations and theory both suggest that $0.25 \lesssim \epsilon_B \lesssim 0.35$, so that the model is well constrained. However, such large values of ϵ_B lead to very efficient initial injection and most of the shock energy is quickly transferred to the CR component for strong shocks considered here ($50 < M_s < 300$ initially), causing a numerical problem at the very early stage of simulations. So we adopted smaller values, $\epsilon_B = 0.16 - 0.2$ in this study. Dependence of the CR injection and acceleration on this parameter will be discussed below.

(d) A Bohm-like Diffusion Model

Self-excitation of Alfvén waves by the CR streaming instability in the upstream region is an integral part of the DAS at SNRs (Bell 1987; Völk *et al.* 1988; Lucek & Bell 2000). The particles are resonantly scattered by those waves, diffuse across the shock, and get injected into the Fermi first-order process. These complex interactions are represented by the diffusion coefficient, which is expressed in terms of a mean scattering length, λ, and the particle speed, v, as $\kappa(x,p) = \lambda v/3$. The Bohm diffusion model is commonly used to represent a saturated wave spectrum (*i.e.*, $\lambda = r_g$, where r_g is

TABLE 1.
MODEL PARAMETERS

Model	$n_{\rm ISM}$ (cm^{-3})	E_o (10^{51} ergs)	B_μ μG	ϵ_B	r_o (pc)	t_o (years)	u_o (10^4 km s^{-1})	P_o (10^{-6}erg cm^{-3})
S1	0.3	1	30	0.16	3.19	255.	1.22	1.05
S2	0.3	4	30	0.16	3.19	127.	2.45	4.20
S3	0.3	1	5	0.16	3.19	255	1.22	1.05
S4	0.003	1	30	0.16	14.8	1182.	1.22	1.05 (-2)
S5	0.3	1	5	0.2	3.19	255	1.22	1.05

the gyro-radius), $\kappa_B(p) = \kappa_n p^2/\ (p^2+1)^{1/2}$. Here $\kappa_n = mc^3/(3eB) = 3.13\times 10^{22}{\rm cm^2 s^{-1}} B_\mu^{-1}$, and B_μ is the magnetic field strength in units of microgauss. Because of the steep momentum dependence for non-relativistic particles ($p \ll 1$), simulations with a Bohm diffusion model require extremely fine grid resolution around the shock where freshly injected CRs are concentrated. Instead we adopt a Bohm-like diffusion coefficient that includes a weaker non-relativistic momentum dependence,

$$\kappa(r,p) = \kappa_{\rm n}\cdot p\left(\frac{\rho_0}{\rho(r)}\right). \qquad (7)$$

Previous studies showed that simulations using these two types of diffusion coefficient produced very similar results (Kang *et al.* 2001). The assumed density dependence for κ accounts for compression of the perpendicular component of the wave magnetic field and also inhibits the acoustic instability in the precursor of highly modified CR shocks (Kang, Jones, & Ryu, 1992). Hereafter we use the subscripts '0', '1', and '2' to denote conditions far upstream of the shock, immediately upstream of the gas subshock and immediately downstream of the subshock, respectively.

III. Simulations of Sedov-Taylor Blast Waves

For a supernova remnant propagating into a uniform ISM, the CR acceleration takes place mostly during free expansion and Sedov-Taylor (ST hereafter) stages, since the shock slows down significantly afterward. Fig. 1 shows the evolution of a typical SNR calculated by a hydrodynamics code without the CR pressure terms. This demonstrates that the ST solution is established only after the inner reverse shock is reflected at the center at $t/t_o \sim 7$ (see below for the definition of normalization constants). Before that time, the reverse shock is strong and dynamically important. In our simulations, however, we will ignore the reverse shock, because the current version of CRASH code can treat only one shock. Application of our AMR algorithm for multiple spherical shocks is not simple, since it requires multiple, comoving grids. The CR acceleration at the reverse shock is thought to be not important, because the kinetic energy passed through the reverse shock is relatively small. Also adiabatic losses by CRs accelerated early on in the interior and then advected outward through the ST phase would generally be very large.

On the other hand, Fig. 1 shows that the evolution of the outer shock speed, $U_{\rm out}(t)$ can be approximated by the Sedov solution $U_{\rm ST}\propto (t/t_o)^{-2/5}$ for $t/t_o > 0.2$. In order to take account for the CR acceleration from free expansion stage through ST stage, we begin the calculations with the ST similarity solution at $t/t_o = 0.5$. In principle we could start the simulations from $t/t_o \sim 0.1$. Such simulations, however, require very long computational time, since we need to include the extremely hot region with fast sound speeds near the explosion center. We carried out one model from $t/t_o = 0.2$ and compared it with the case started from $t/t_o = 0.5$ in the next section. Since the total CR energy gain is proportional to the kinetic energy passed through the shock, $E_{sw} = 2\pi\int \rho_0 U_{\rm out}^3 R_{\rm out}^2 dt$, we expect our calculations should capture the key aspects of the CR acceleration at the outer SNR shock.

We terminated the simulation at $t/t_o = 10$, while the ST stage ends typically when the shock slows down to $U_{\rm ST} < 300$ km s^{-1} around $t/t_o \sim 3000$. However, it has been shown that the highest momentum, $p_{\rm max}$, is achieved by the end of the free expansion stage and the transfer of explosion energy to the CR component occurs mostly during the early ST stage (*e.g.,* Berezhko *et al.* 1997). We will show in the next section that the shock properties and the CR acceleration efficiency reach roughly time asymptotic values for $t/t_o > 1$. Also it was suggested that non-linear wave damping and the wave dissipation due to ion-neutral collisions may suppress the MHD waves significantly at the late ST stage, leading to fast particle diffusion and inefficient acceleration. (Völk *et al.* 1998; Ptuskin & Zirakashvili 2003)

IV. Results

(a) SNR Model Parameters

We consider a Type Ia supernova explosion with the ejecta mass, $M_{ej} = 1.4 M_\odot$, in a warm or hot ISM with a uniform density. Model parameters are summarized in Table 1. The fiducial model, labeled S1 in Table 1, has the explosion energy, $E_o = 10^{51}$ ergs, and the background density, $n_{\rm ISM} = 0.3$ cm^{-3}. The pressure of the

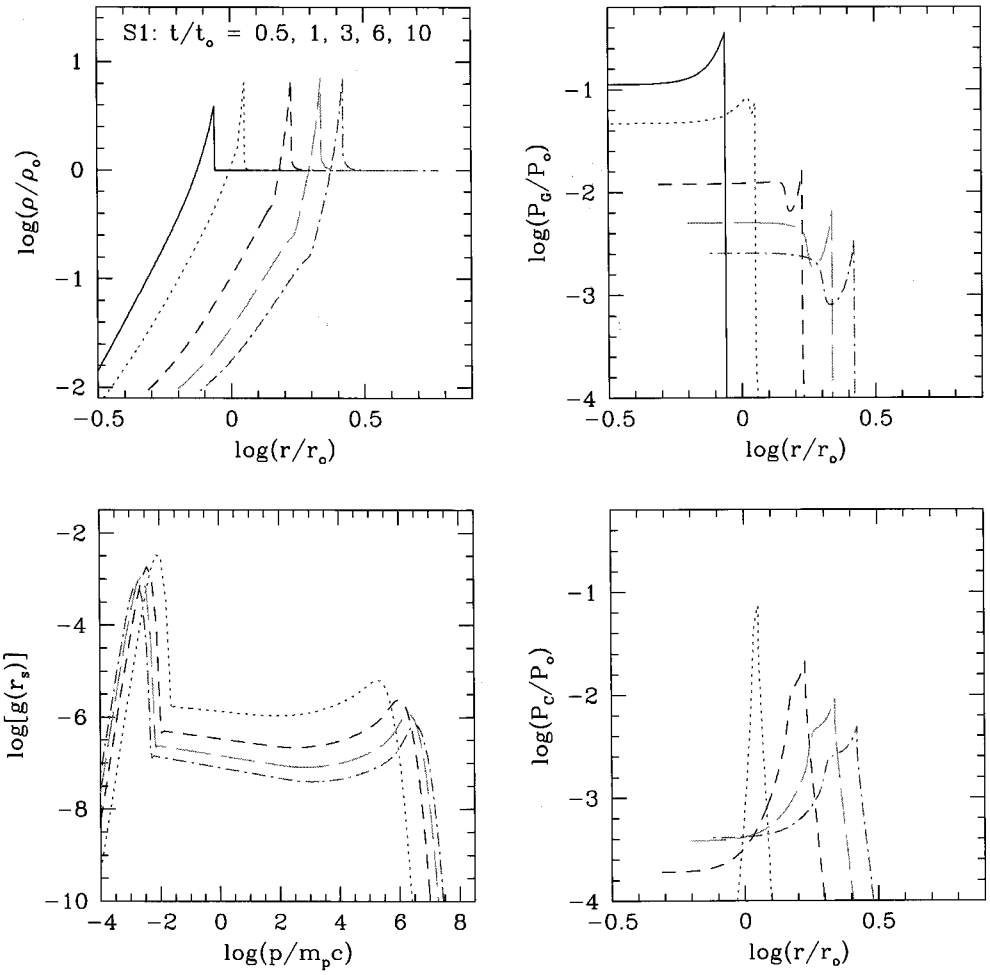

Fig. 2.— Evolution of model S1 SNR expanding into a uniform ISM at $t/t_o = 0.5$, 1., 6., and 10. The model parameters are $M_{ej} = 1.4M_\odot$, $E_o = 10^{51}$ ergs, $n_{\rm ISM} = 0.3{\rm cm}^{-3}$, and $B_\mu = 30$. The injection parameter for thermal leakage injection, $\epsilon_B = 0.2$. The lower left panel shows the volume integrated CR spectrum, $G(p) = \int f(r,p)p^4r^2{\rm dr}$. The initial condition at $t/t_o = 0.5$ (solid line) is set by the Sedov-Taylor similarity solution.

background gas is set to be $P_{\rm ISM} \approx 10^{-12}$ erg cm^{-3}, which determines the sound speed of the upstream gas and so the Mach number of the SNR shock. Recent X-ray observations of young SNRs indicate a magnetic field strength much greater than the mean ISM field of 5μG, or values expected by compression of that field (*e.g.*, Berezhko *et al.* 2003; Völk *et al.* 2005). It is believed that the magnetic field upstream from the shock is amplified by the CR streaming instability in the precursor region (Bell 1978, Lucek & Bell 2000). Thus, to represent this effect we take $B = 30\mu$G as the fiducial field strength. The strength of magnetic field determines the size of diffusion coefficient, κ_n, and the drift speed of Alfvén waves relative to the bulk flow. The Alfvén speed is given by $v_A = v_{A,0}(\rho/\rho_0)^{-1/2}$ where $v_{A,0} = (1.8\ {\rm kms}^{-1})B_\mu/\sqrt{n_{\rm ISM}}$. The second model, S2, assumes a higher explosion energy, while the third model, S3, assumes the ISM magnetic field, rather than the amplified field. Model S4 assumes a hot ISM ($T \approx 10^6$ K), while all other models assume a warm ISM ($T \approx 10^4$ K). For models S1-S4 $\epsilon_B = 0.16$ is adopted. Model S5 has the same parameters as model S3 except $\epsilon_B = 0.2$, which allows a higher injection rate.

The physical quantities are normalized, both in the numerical code and in the plots below, by the following constants:

$$r_o = \left(\frac{3M_{ej}}{4\pi\rho_o}\right)^{1/3},$$

$$t_o = \left(\frac{\rho_o r_o^5}{E_o}\right)^{1/2},$$

$$u_o = r_o/t_o,$$

$$\rho_o = (2.34\times10^{-24}{\rm gcm}^{-3})n_{\rm ISM},$$

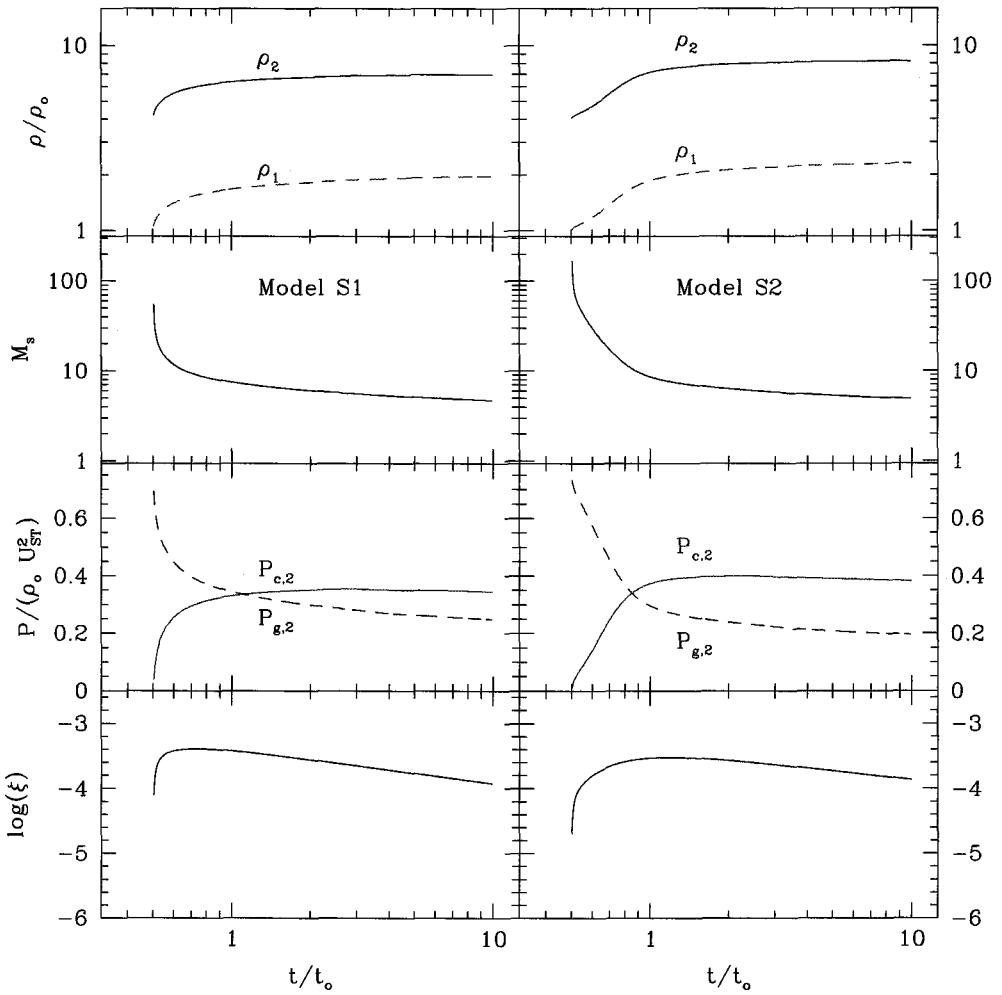

Fig. 3.— Immediate pre-subshock density, ρ_1, post-subshock density, ρ_2, shock Mach number, M_s, post-subshock CR and gas pressure in units of the ram pressure of the unmodified Sedov-Taylor solution, $\rho_0 U_{ST}^2 \propto (t/t_o)^{-6/5}$, and the CR injection parameter, ξ, are plotted for models S1 and S2.

$$P_o = \rho_o u_o^2.$$

These values are also given in Table 1 for reference.

(b) Remnant Evolution

Fig. 2 shows the evolution of model S1 for $t/t_o = 0.5 - 10$. The solid lines are for the initial condition which is assumed be the Sedov Taylor similarity solution ($R_{\rm ST}/r_o = \xi_s(t/t_o)^{0.6}$, $U_{\rm ST}/u_o = 0.6\xi_s(t/t_o)^{-0.4}$, where $\xi_s = 1.15167$) extrapolated to $t/t_o = 0.5$. Initially there is no pre-existing CRs and so all CR particles are freshly injected at the shock. The CR pressure becomes dominated over the gas pressure and the density compression across the total shock becomes $\rho_2/\rho_0 \approx 7$ after $t/t_o \sim 1$. As the shock slows down and the CR pressure increases, the subshock Mach number decreases and the thermal population cools down, resulting in less efficient particle injection at low energies. We note that the inner boundary of the simulation grid moves out with the expanding comoving grid.

We repeated the same calculation starting from an earlier time, $t/t_o = 0.2$, to explore how the CR acceleration during the early free expansion stage would affect the results at late ST stage. The total CR energy accelerated by $t/t_o = 10$ differs about 3 % and the CR spectrum extends to slightly higher $p_{\rm max}$ in the simulation started from $t/t_o = 0.2$, as one would anticipate from the longer acceleration interval. The small differences indicate that omitting the evolution before $t/t_o = 0.5$ does not affect the overall conclusions of this work.

(c) CR Injection and Acceleration

The efficiency of the particle injection is quantified by the fraction of particles swept through the shock

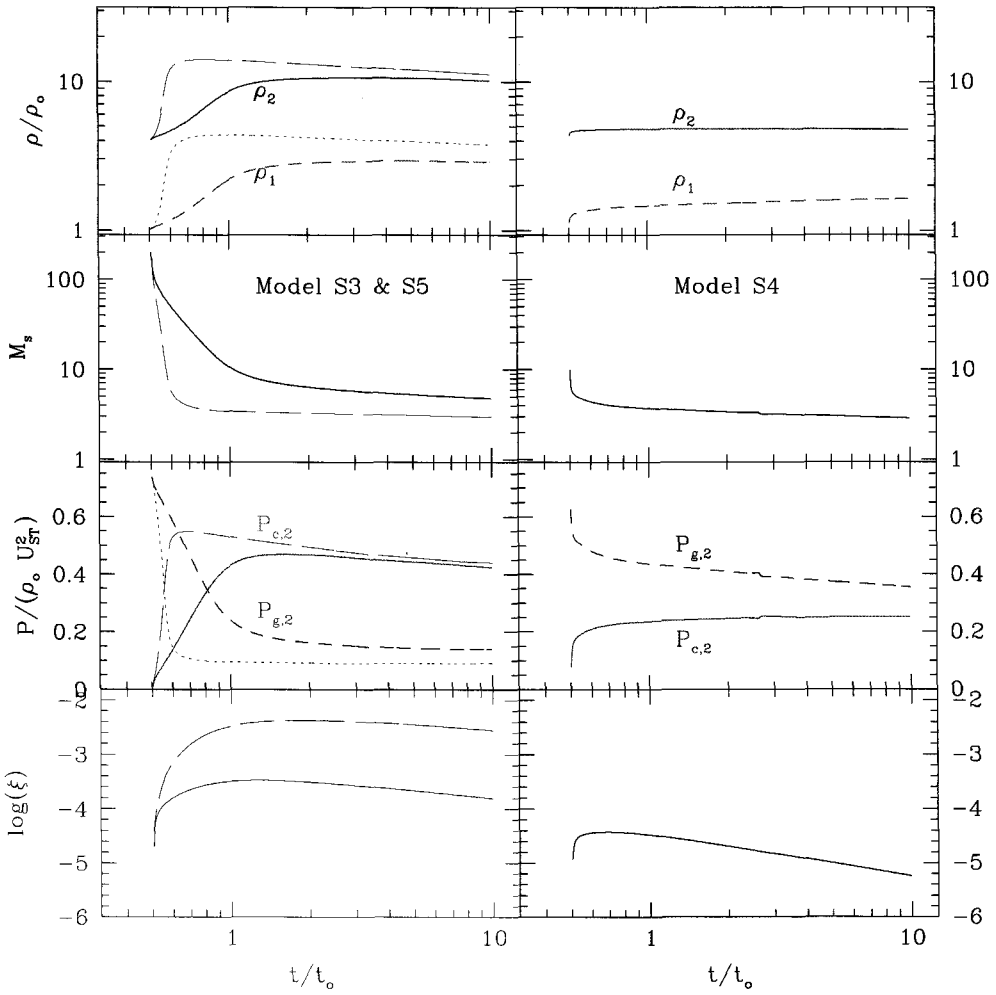

Fig. 4.— Pre-subshock density, ρ_1, post-subshock density, ρ_2, shock Mach number, M_s, post-subshock CR and gas pressure in units of the ram pressure of the unmodified Sedov-Taylor solution, $\rho_0 U_{ST}^2 \propto (t/t_o)^{-6/5}$, and the CR injection parameter, ξ, are plotted for models S3 and S4. The left panels also show model S5 with $\epsilon_B = 0.2$ (long dashed lines and dotted lines).

that have been injected into the CR distribution:

$$\xi(t) = \frac{\int 4\pi r^2 \mathrm{dr} \int 4\pi f_{\mathrm{CR}}(p,r,t) p^2 \mathrm{dp}}{\int 4\pi r_s^2 n_0 u_s \mathrm{dt}}, \qquad (8)$$

where f_{CR} is the CR distribution function, n_0 is the particle number density far upstream and r_s is the shock radius.

Figs. 3-4 show the evolution of shock properties such as the compression factors, subshock Mach number, postshock pressures, and the injection fraction for all five models. Most of these quantities approach to time-asymptotic values. The shock Mach number is the key parameter that determines the CR injection and acceleration efficiency. Model S4 has much lower initial Mach number, so it shows less injection rate ($\xi \sim 10^{-5}$) compared to the other models ($\xi \gtrsim 10^{-4}$). The compression factor in the precursor, $\rho_1/\rho_0 \approx 2-3$, while the compression factor across the total shock structure varies somewhat, $\rho_2/\rho_0 \approx 7.0$, 8.2, 10., and 4.8 for models S1-S4, respectively. The postshock CR pressure relative to the ram pressure of the Sedov solution is $P_{c,2}/\rho_0 U_{ST}^2 \approx 0.35$, 0.39, 0.42, and 0.25 for models S1-S4, respectively.

We note that model S4 with $B = 5\mu$G has the higher CR pressure than the fiducial model S1 with $B = 30\mu$G. While the mode with higher B has smaller diffusion coefficient and so the CR spectrum extends to higher p_{max} (see Fig. 5), the reduction of the injection and acceleration due to the wave drift leads to less CR energy.

Model S5 has a larger value of $\epsilon_B = 0.2$ than model S3 does, but otherwise they have the same model parameters. Weaker turbulence (larger ϵ_B) lead to higher thermal leakage, so the injection rate ξ is about 15 times larger than that of models S1-S3. This in turn results in slightly higher CR pressure and more significant precursor compression. However, it demonstrates that the CR acceleration efficiency depends only weakly

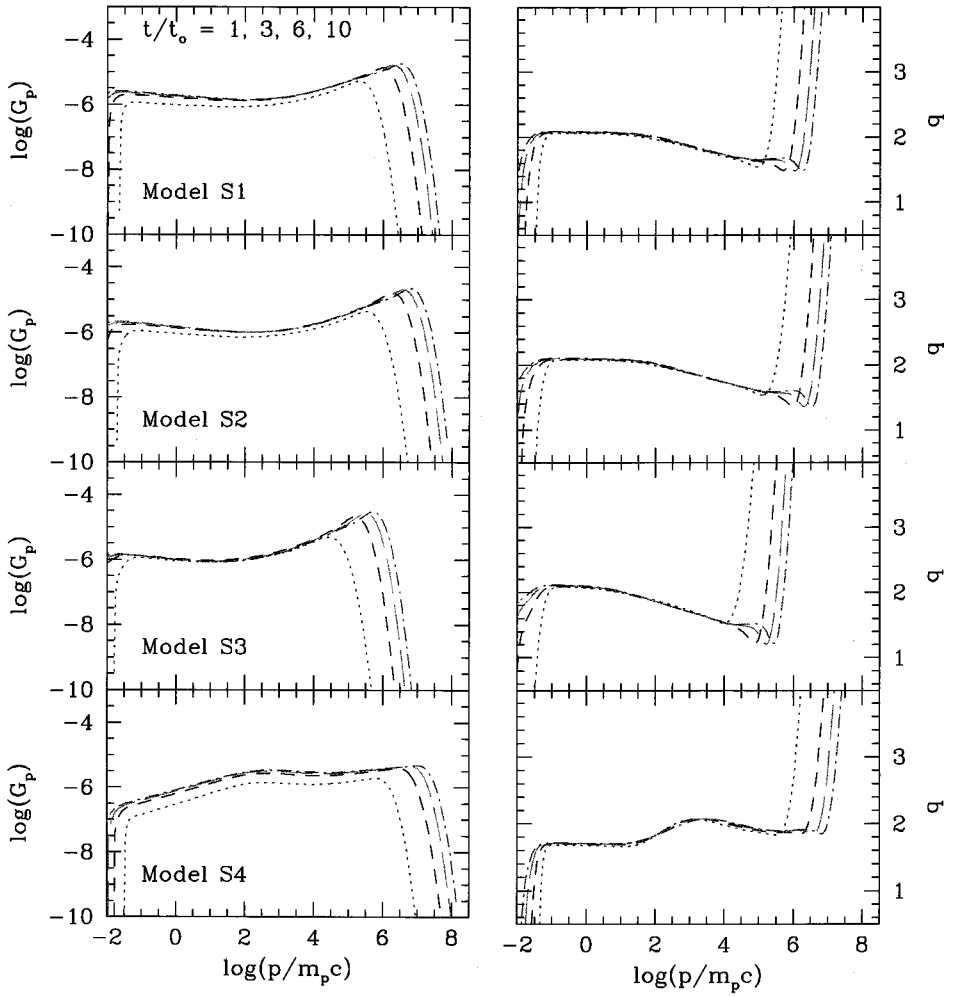

Fig. 5.— Integrated CR number, $G_p = \int g(p) r^2 \mathrm{d}r$, in arbitrary units and the slope, $q = -d(\ln G_p)/d\ln p - 2$, are shown at $t/t_o = 1$, 3, 6, and 10. See Table 1 for model parameters for models S1-4.

on the injection rate.

Fig. 5 shows the volume integrated CR spectrum, $G(p) = \int 4\pi g(p) r^2 \mathrm{d}r$ in code units and the slope, $q = -d(\ln G_p)/d\ln p - 2$. The maximum momentum depends on the SNR parameters as $p_{\max} \propto u_s^2 t/\kappa_n \propto B_\mu E_o \rho_{\rm ISM}^{-1/3}$. The values of $\log(p_{\max}) \approx 6.5$, 6.8, 5.7, and 7.0 at $t/t_o = 10$ for models S1-S4, respectively, are roughly consistent with this relation.

The CR spectra for models S1-S3 with high initial Mach numbers show the canonical nonlinear concave curvature for $p \gg 1$, which comes from the large density compression factor ($\rho_2/\rho_0 \gg 4$) due to the dominant CR pressure. For these models the slope q is close to 2 at low energies, but flattens to ~ 1.6 at high energies below the upper momentum cutoff. For model S4 with lower initial Mach number the density compression is only $\rho_2/\rho_0 \approx 4.8$, so the flattening of $G(p)$ at high momenta is not so prominent. Instead, the decrease of the CR injection rate due to the weakening subshock reduces the particle numbers at low momentum, leading to actually flatter spectra there.

Fig. 6 shows the integrated energies, $E_i/E_o = 4\pi \int e_i r^2 \mathrm{d}r$, where e_{th}, e_{kin}, and e_C are the density of thermal, kinetic and cosmic ray energy, respectively. The kinetic energy reduces only slightly and is similar for all models. The total CR energy accelerated up to $t/t_o = 10$ is $E_C/E_o = 0.55$, 0.57, 0.62 and 0.39 for models S1-S4, respectively. So models S2 (larger E_o) and S3 (smaller B_μ) are a bit more efficient in transferring the SN explosion energy to the CR energy, compared to the fiducial model. As mentioned earlier, comparison between models S1 and S3 indicates that strongly amplified magnetic field carries faster Alfvén waves and leads to less efficient CR acceleration, even though the particles are accelerated to higher energies. Also comparison between models S3 and S5 shows that the total CR energy increases only slightly, less than 3 %, even though the injection rate increases by a factor of about 15 with a larger value of ϵ_B for model S5. In model S4

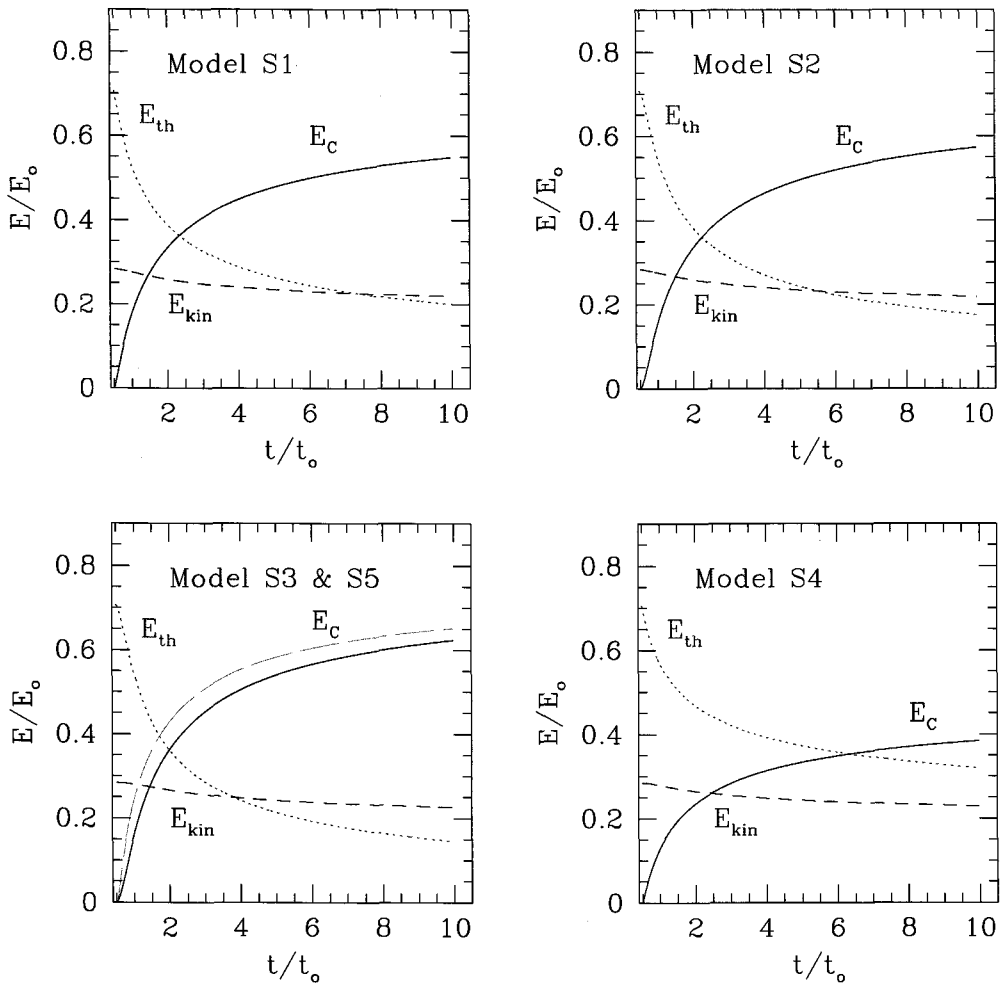

Fig. 6.— Integrated thermal, kinetic and CR energies inside the simulation volume as a function of time. See Table 1 for model parameters for models S1-S5. The long dashed line in the lower left panel shows the volume integrated CR energy for model S5.

with a hotter ISM, the shock is weaker and so the CR injection and acceleration are less efficient.

Our simulations imply that on average about $10^{-4}-10^{-3}$ of the incoming particles are injected to the CR population at the shock front and up to 50 % of the SN explosion energy can be transferred to CRs during the ST stage, if the magnetic field direction is radial (*i.e.*, quasi-parallel field). This last result is consistent with the calculations previously done by Berezhko and collaborators using a different numerical scheme (*e.g.*, Berezhko & Völk 1997). The CR injection rate, however, probably depends strongly on the angle between the magnetic field and the shock normal direction. In a more realistic magnetic field geometry, where a uniform ISM field is swept by the spherical shock, only 10-20 % of the shock surface has a quasi-parallel field geometry (Völk *et al.* 2003). In the shock surface region where the field is perpendicular, the injection rate is expected to be reduced and so the CR acceleration efficiency would be smaller. Thus the CR energy conversion factor averaged over the entire shock surface could be significantly smaller than 50 %, perhaps about 10 %. On the other hand, Giacolne (2005) showed that the protons can be injected efficiently even at perpendicular shocks in fully turbulent fields due to field line meandering. In such case the injection rate at perpendicular shocks may not be significantly smaller, compared to parallel shocks.

V. SUMMARY

The evolution of cosmic ray modified shocks depends on complex interactions between the particles, waves in the magnetic field, and underlying plasma flow. We have developed numerical tools that can emulate some of those interactions and incorporated them into a standard numerical scheme for gasdynamic problems. Specifically, diffusive shock acceleration can be followed by a kinetic approach (*i.e.*, CRASH code) in

which a diffusion convection equation for the CR distribution function is solved with an appropriate diffusion coefficient (Kang & Jones 1991; Kang *et al.* 2001). The injection of CR particles can be treated by a thermal leakage injection model with a transparency function $\tau_{\rm esc}(\epsilon_B, v)$ (Kang *et al.* 2002). Drifts of resonantly-scattering Alfvén waves and heating of the thermal plasma due to the dissipation of those waves in the precursor region has been included through a simple model (Jones 1993; Kang & Jones 2006).

In the present paper, we applied the spherical CRASH code to the problem of the CR acceleration at the remnant shock from typical Type Ia SNe propagating into a uniform interstellar medium. The main results of our simulations can be summarized as follows:

1) Since the CR injection and acceleration depend primarily on the shock Mach number, the temperature of the ISM is an important factor. SNRs in a warm ISM inject about $10^{-4} - 10^{-3}$ of the particles passed through the shock and transfer about 50% of the explosion energy to the CR component. SNRs in a hot ISM inject 10 times less particles, but they still transfer about 40 % of the explosion energy to CRs.

2) At sources, the hadronic CR spectrum should be consistent with a power-law function, $N(E)dE \propto E^{-2}dE$ up to $p/m_{\rm p}c \sim 10^2$, but it may gradually flatten to $E^{-1.6}$ toward the Knee energy and beyond up to $E \sim 10^{16}Z$ eV ($p/m_{\rm p}c \sim 10^7$).

3) About 40-50 % of the explosion energy can be transfered to CRs, if the magnetic field is radial (*i.e.,* quasi-parallel shocks). However, more realistic consideration of the field geometry relative to the spherical shock surface could lead to much smaller energy conversion rate. So a conservative estimate could be order of 10 %.

4) If the magnetic field is amplified in the precursor region due to the streaming instability, as indicated by recent X-ray observations of young SNRs, the particles are accelerated to higher energies due to smaller diffusion coefficient. However, faster Alfvén waves in the precursor tend to reduce the CR injection and acceleration efficiencies.

In conclusion, the galactic cosmic rays possibly up to $10^{16}Z$ eV could be originated from supernova remnants. This result is quite robust, regardless of SNR model parameters and details of microphysics involved in the injection process, provided that the Bohm diffusion is valid at young SNRs of several thousand years old.

ACKNOWLEDGEMENTS

This work was supported for two years by Pusan National University Research Grant. The author would like to thank T.W. Jones for helpful comments on the paper.

REFERENCES

Aharonian, F. A *et al.* , H.E.S.S. collaboration, 2004, High-energy particle acceleration in the shell of a supernova remnant, Nature, 432, 75

Bamba, A., Yamazaki, R, Ueno, M. & Koyama, K., 2003, Small-Scale Structure of the SN 1006 Shock with Chandra Observations, ApJ, 589, 827

Bell, A. R., 1978, The acceleration of cosmic rays in shock fronts. I, MNRAS, 182, 147

Berezhko, E. G., Ksenofontov, L. T., & Yelshin, V., 1995, Efficiency of CR acceleration in supernova remnants, Nuclear Physic B., 39, 171.

Berezhko, E. G., & Völk, H. J., 1997, Kinetic theory of cosmic rays and gamma rays in supernova remnants. I. Uniform interstellar medium, Astropart. Phys. 7, 183

Berezhko, E. G., Ksenofontov, L. T., & Völk, H. J., 2003, Confirmation of strong magnetic field amplification and nuclear cosmic ray acceleration in SN 1006, A&Ap, 423, L11

Berezhko, E. G., & Völk, H. J., 2006, Theory of cosmic ray production in the supernova remnant RX J1713.7-3946, A&Ap, 451, 981

Blandford, R. D., & Ostriker, J. P., 1978, Particle acceleration by astrophysical shocks, ApJ, 221, L29

Blandford, R. D., & Eichler, D., 1987, Particle acceleration at astrophysical shocks - a theory of cosmic-ray origin, Phys. Rept., 154, 1

Drury, L. O'C., 1983, An Introduction to the Theory of Shock Acceleration of Energetic Particles in Tenuous Plasmas, Rept. Prog. Phys., 46, 973

Drury, L. O'C., Ellison, D. E., Aharonian, F. A. *et al.* ,2001, Test of galactic cosmic-ray source models - Working Group Report, Space Science Reviews, 99, 329

Giacalone, J., 2005, The Efficient Acceleration of Thermal Protons by Perpendicular Shocks ApJ, 628, L37

Jones, T. W., 1993, Alfvén wave transport effects in the time evolution of parallel cosmic-ray-modified shocks ApJ, 413, 619

Kang, H., & Jones, T. W., 1991, Numerical studies of diffusive particle acceleration in supernova remnants, MNRAS, 249, 439

Kang, H., Jones, T. W., & Ryu, D., 1992, Acoustic instability in cosmic ray mediated shocks, ApJ, 385, 193

Kang, H., Jones, T. W., LeVeque, R. J., & Shyue, K. M., 2001, Time Evolution of Cosmic-Ray Modified Plane Shocks, ApJ, 550, 737

Kang, H., Jones, T. W., & Gieseler, U. D. J., 2002, Numerical Studies of Cosmic-Ray Injection and Acceleration, ApJ, 579, 337

Kang, H., & Jones, T. W., 2002, Acceleration of Cosmic Rays at Large Scale Cosmic Shocks in the Universe, Journal of Korean Astronomical Society, 35, 159

Kang, H., 2003, Cosmic Ray Acceleration at Cosmological Shocks: Numerical Simulations of CR Modified Plane-Parallel Shocks Journal of Korean Astronomical Society, 36, 1

Kang, H., & Jones, T. W., 2006, Numerical studies of diffusive shock acceleration at spherical shocks Astropart. Phys. 25, 246

Koyama, K., Petre, R., Gotthelf, E. V. *et al.* ,1995, Evidence for Shock Acceleration of High-Energy Electrons in the Supernova Remnant SN:1006, Nature, 378, 255

Lagage, P. O., & Cesarsky, C. J., 1983, The maximum energy of cosmic rays accelerated by supernova shocks, A&Ap, 118, 223

Lucek, S. G., & Bell, A. R., 2000, Non-linear amplification of a magnetic field driven by cosmic ray streaming, MNRAS, 314, 65

Malkov, M. A., & Drury, L. O'C., 2001, Nonlinear theory of diffusive acceleration of particles by shock waves, Rep. Progr. Phys. 64, 429

Malkov, M. A., & Völk, H. J., 1998, Diffusive ion acceleration at shocks: the problem of injection, Adv. Space Res. 21, 551

Ptuskin, V. S., & Zirakashvili, V. N., 2003, Limits on diffusive shock acceleration in supernova remnants in the presence of cosmic-ray streaming instability and wave dissipation, A&Ap, 403, 1

Skilling, J., 1975, Cosmic ray streaming. I - Effect of Alfvén waves on particles, MNRAS, 172, 557

Völk, H. J., Berezhko, E. G., & Ksenofontov, L. T., 2003, Variation of cosmic ray injection across supernova shocks, A&Ap, 409, 563

Völk, H. J., Berezhko, E. G., & Ksenofontov, L. T., 2005, Magnetic field amplification in Tycho and other shell-type supernova remnants A&Ap, 433, 229

Völk, H. J., Zank, L. A., & Zank, G. P., 1988, Cosmic ray spectrum produced by supernova remnants with an upper limit on wave dissipation, A&Ap, 198, 274